Unified Constant-Frequency Integration Control of Three-Phase Standard Bridge Boost Rectifiers With Power-Factor Correction

Chongming Qiao, *Student Member, IEEE,* and Keyue M. Smedley, *Senior Member, IEEE*

***Abstract*—In this paper, a three-phase six-switch standard boost rectifier with unity-power-factor correction is investigated. A general equation is derived that relates the input phase voltages, output dc voltage, and duty ratios of the switches in continuous conduction mode. Based on one of the solutions and using one-cycle control, a unified constant-frequency integration controller for PFC is proposed. For the standard bridge boost rectifier, a unity power factor and low total harmonic distortion can be realized in all three phases with a simple circuit that is composed of one integrator with reset along with several flips-flops, comparators, and some logic and linear components. It does not require multipliers and three-phase voltage sensors, which are required in many other control approaches. In addition, it employs constant-switching-frequency modulation that is desirable for industrial applications. The proposed control approach is simple and reliable. All findings are supported by experiments.**

***Index Terms*—One-cycle control, power-factor correction (PFC), power quality control, three-phase rectifier.**

I. Introduction

TRADITIONAL diode rectifiers and thyristor rectifiers draw pulsed current from the ac main, causing significant current harmonics pollution, elevated power rating, and harmonic/reactive power losses. The international standards presented in IEC 1000–3-2 and EN61000–3-2 imposed harmonic restrictions to modern rectifiers, which have resulted in a focused research effort on the topic of unity-power-factor rectifiers. Three-phase power-factor-correction (PFC) rectifiers are preferred for high-power applications due to their symmetric current-drawing characteristics. Many topologies have been proposed recently [1]–[4]. Among them, the six-switch bridge boost rectifier is a commonly used topology. In the previously proposed rectifiers, hysteresis control and d–q transformation control were frequently used to control six-switch bridge boosts. Hysteresis control results in variable switching frequency, which can cause difficulties for electromagnetic interference (EMI) filter design. The d–q approach leads to complicated systems. An encouraging analog solution, with constant switching frequency modulation, was provided in [5] for a six-switch bridge boost rectifier. However, three-phase voltage is sensed for the six-step operation and multipliers are necessary to implement the three-phase current references.

In this paper, a general equation that relates input phase voltages, output dc voltage, and duty ratios of switches is derived for the six-switch bridge boost rectifier based on an average model in continuous conduction mode (CCM). This equation of the average model is singular and has infinite solutions. Based on the one-cycle control concept [6]–[10] and one solution of this general equation, a unified constant-frequency integration (UCI) controller is introduced that realizes three-phase unity power factor and low total harmonic distortion (THD). The proposed controller features the following:

- constant switching frequency;
- no need for the multipliers that are required to scale the current reference, according to load level, as used in many other control approaches;
- three-phase voltage sensors are eliminated;
- only one integrator with reset, along with some logic and linear components, is required; it is simple and reliable.

II. Proposed UCI Controller

The analysis in this section is based on following assumptions.

- The switches in each arm operate in a complementary fashion, e.g., the duty ratios for switches S_{an}, S_{ap} are d_{an} and $1-d_{an}$ respectively, etc.
- Three-phase system is symmetrical.
- Switching frequency is much higher than line frequency.

A six-switch standard bridge boost rectifier is shown in Fig. 1(a). The average voltages at the nodes A, B, and C, referred to node N, are given by

$$\begin{cases} v_{AN} = (1-d_{an})\cdot E \\ v_{BN} = (1-d_{bn})\cdot E \\ v_{CN} = (1-d_{cn})\cdot E \end{cases} \tag{1}$$

where d_{an}, d_{bn}, and d_{cn} are the duty ratios for switches S_{an}, S_{bn}, and S_{cn}. The equivalent average model for the rectifier in Fig. 1(a) is shown in Fig. 1(b). The average vector voltage at nodes A, B, and C, referred to the neutral point "O," equal the phase vector voltages minus the voltage across the inductors L_a, L_b, and L_c, as given by

$$\begin{cases} \dot{v}_{AO} = \dot{v}_a - jwL\cdot\dot{i}_{La} \\ \dot{v}_{BO} = \dot{v}_b - jwL\cdot\dot{i}_{Lb} \\ \dot{v}_{CO} = \dot{v}_c - jwL\cdot\dot{i}_{Lc} \end{cases} \tag{2}$$

Manuscript received February 19, 2001; revised March 15, 2002. Abstract published on the Internet September 13, 2002. This paper was presented at the 7th IEEE International Power Electronics Congress (CIEP 2000), Acapulco, Mexico, October 15–19, 2000.

The authors are with the Department of Electrical and Computer Engineering, University of California, Irvine, CA 92697 USA (e-mail: smedley@ uci.edu).

Digital Object Identifier 10.1109/TIE.2002.804980

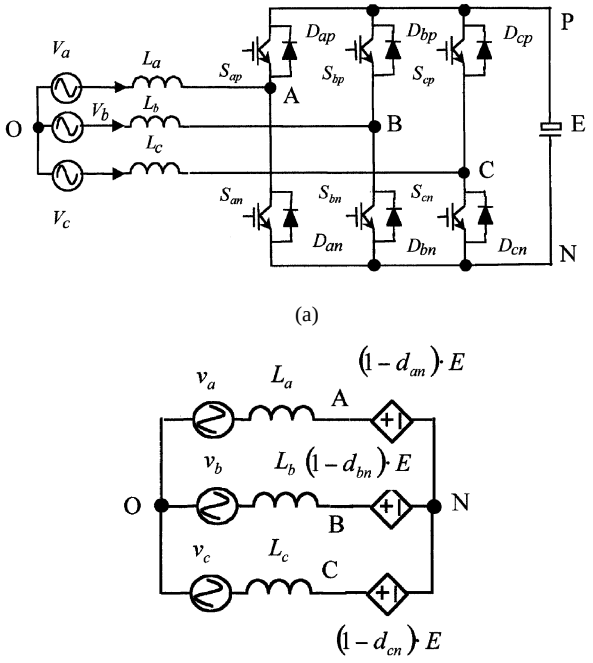

Fig. 1. (a) Three-phase six-switch bridge boost rectifier. (b) Average model.

where L is the inductance of input inductors (assuming the three-phase inductors are identical), w is the line angular frequency, and $\vec{i}_{La}$, $\vec{i}_{Lb}$, and $\vec{i}_{Lc}$ are the inductor current vectors. Since these inductors are operating at high frequency, and the inductance L is very small as regards a 60-Hz utility system, the voltages across the inductors, such as $jwL \cdot \vec{i}_{La}$, are very small, compared to the phase voltage, and may be neglected. Therefore, (2) can be simplified as

$$\begin{cases} \dot{v}_{AO} \approx \dot{v}_a \\ \dot{v}_{BO} \approx \dot{v}_b \\ \dot{v}_{CO} \approx \dot{v}_c \end{cases} \Rightarrow \begin{cases} v_{AO} \approx v_a = \sqrt{2}V_i \cdot \sin(wt) \\ v_{BO} \approx v_b = \sqrt{2}V_i \cdot \sin(wt - 120^\circ) \\ v_{CO} \approx v_c = \sqrt{2}V_i \cdot \sin(wt + 120^\circ) \end{cases}. \tag{3}$$

For a symmetric three-phase system, it holds that

$$v_a + v_b + v_c = 0. \tag{4}$$

This leads to

$$v_{AO} + v_{BO} + v_{CO} = 0. \tag{5}$$

The voltages at nodes A, B, and C, referred to the neutral point, are given by

$$\begin{cases} v_{AO} = v_{AN} + v_{NO} \\ v_{BO} = v_{BN} + v_{NO} \\ v_{CO} = v_{CN} + v_{NO}. \end{cases} \tag{6}$$

Combining (5) and (6) yields

$$v_{NO} = -\frac{1}{3} \cdot (v_{AN} + v_{BN} + v_{CN}). \tag{7}$$

Substituting (7) and (3) into (6) results in

$$\begin{cases} v_{AO} = v_{AN} - \frac{1}{3} \cdot (v_{AN} + v_{BN} + v_{CN}) \approx v_a \\ v_{BO} = v_{BN} - \frac{1}{3} \cdot (v_{AN} + v_{BN} + v_{CN}) \approx v_b \\ v_{CO} = v_{CN} - \frac{1}{3} \cdot (v_{AN} + v_{BN} + v_{CN}) \approx v_c. \end{cases} \tag{8}$$

Simplification yields

$$\begin{bmatrix} \frac{2}{3} & -\frac{1}{3} & -\frac{1}{3} \\ -\frac{1}{3} & \frac{2}{3} & -\frac{1}{3} \\ -\frac{1}{3} & -\frac{1}{3} & \frac{2}{3} \end{bmatrix} \cdot \begin{bmatrix} v_{AN} \\ v_{BN} \\ v_{CN} \end{bmatrix} = \begin{bmatrix} v_a \\ v_b \\ v_c \end{bmatrix}. \tag{9}$$

The combination of (1) and (9) yields the relationship between duty ratio d_{an}, d_{bn}, d_{cn} and voltage v_a, v_b, v_c, which is shown as follows:

$$\begin{bmatrix} -\frac{2}{3} & \frac{1}{3} & \frac{1}{3} \\ \frac{1}{3} & -\frac{2}{3} & \frac{1}{3} \\ \frac{1}{3} & \frac{1}{3} & -\frac{2}{3} \end{bmatrix} \cdot \begin{bmatrix} d_{an} \\ d_{bn} \\ d_{cn} \end{bmatrix} = \frac{1}{E} \cdot \begin{bmatrix} v_a \\ v_b \\ v_c \end{bmatrix}. \tag{10}$$

This equation relates the average duty ratio of switches to the line voltage. Since the matrix of (10) is singular, (10) has no unique solution. One possible solution for (10) is as follows:

$$\begin{cases} d_{an} = K_1 + K_2 \cdot \frac{v_a}{E} \\ d_{bn} = K_1 + K_2 \cdot \frac{v_b}{E} \\ d_{cn} = K_1 + K_2 \cdot \frac{v_c}{E}. \end{cases} \tag{11}$$

Substituting the above equation into (10) results in the following: parameter $K_2 = -1$ and K_1 can be any number. Because the duty ratio is less than unity and greater than zero, the following limitation holds:

$$0 \le d_{an} = K_1 - \frac{v_a}{E} \le 1. \tag{12}$$

The parameter K_1 is limited by

$$\frac{v_a}{E} \le K_1 \le 1 + \frac{v_a}{E}. \tag{13}$$

Equation (11) can be rewritten as

$$\begin{cases} \frac{v_a}{E \cdot K_1} = 1 - \frac{d_{an}}{K_1} \\ \frac{v_b}{E \cdot K_1} = 1 - \frac{d_{bn}}{K_1} \\ \frac{v_c}{E \cdot K_1} = 1 - \frac{d_{cn}}{K_1}. \end{cases} \tag{14}$$

For an ideal three-phase rectifier with unity power factor, the three-phase currents should follow the three-phase sinusoidal voltages. Therefore, the impedance looking into the three-phase rectifier from the utility side should be resistive. Define R_e as the emulated resistance, where the size of R_e reflects the power flowing into the rectifier. The control goal is to realize the following relationship between the input voltages and currents:

$$\begin{cases} v_a = R_e \cdot i_a \\ v_a = R_e \cdot i_a \\ v_a = R_e \cdot i_a. \end{cases} \tag{15}$$

Combining the above equation and (14) yields

$$\begin{cases} \frac{R_e}{E\cdot K_1\cdot R_S}\cdot R_S\cdot i_a = 1-\frac{d_{an}}{K_1} \\ \frac{R_e}{E\cdot K_1\cdot R_S}\cdot R_S\cdot i_b = 1-\frac{d_{bn}}{K_1} \\ \frac{R_e}{E\cdot K_1\cdot R_S}\cdot R_S\cdot i_c = 1-\frac{d_{cn}}{K_1} \end{cases} \tag{16}$$

where parameter R_s is the equivalent current-sensing resistor. Define

$$V_m = \frac{E\cdot R_s\cdot K_1}{R_e} \tag{17}$$

where V_m is the output of the feedback error compensator. Equation (16) can be simplified as

$$\begin{cases} R_s\cdot i_a = V_m - V_m\cdot\frac{d_{an}}{K_1} \\ R_s\cdot i_b = V_m - V_m\cdot\frac{d_{bn}}{K_1} \\ R_s\cdot i_c = V_m - V_m\cdot\frac{d_{cn}}{K_1}. \end{cases} \tag{18}$$

Three-phase PFC can be achieved by controlling the switches in such a way that the duty ratios and input currents satisfy (18). Assuming that the input inductor currents operate in the CCM with small ripple, in each switching cycle, the average inductor current, which equals phase current, is approximately equal to the peak inductor current in each switching cycle, that is,

$$\begin{cases} i_a = \langle i_{La}\rangle \approx i_{Lapk} \\ i_b = \langle i_{Lb}\rangle \approx i_{Lbpk} \\ i_c = \langle i_{Lc}\rangle \approx i_{Lcpk} \end{cases}$$

where $\langle i_{La}\rangle$, $\langle i_{Lb}\rangle$, and $\langle i_{Lc}\rangle$ are inductor cycle average currents and i_{Lapk}, i_{Lbpk}, and i_{Lcpk} are inductor peak currents during each switching cycle. The control key equations for peak inductor current sensing are derived as

$$\begin{cases} R_s\cdot i_{Lapk} = V_m - V_m\cdot\frac{d_{an}}{K_1} \\ R_s\cdot i_{Lbpk} = V_m - V_m\cdot\frac{d_{bn}}{K_1} \\ R_s\cdot i_{Lcpk} = V_m - V_m\cdot\frac{d_{cn}}{K_1}. \end{cases} \tag{19}$$

The above equation can be implemented by the one-cycle control circuit, i.e., an integrator with reset, together with some linear and logic components. The overall schematic for the proposed three-phase UCI PFC controller with peak inductor current sensing is shown in Fig. 2(a). No voltage sensors and multipliers are required. The operational waveforms are shown in Fig. 2(b), where $Q_{ap}, Q_{an}\ldots Q_{cn}$ are the driver signals for switches $S_{ap}, S_{an}\ldots S_{cn}$, respectively.

In the beginning of each switching cycle, the clock sets the output of flip-flops to high, Q_{ap}, Q_{bp}, Q_{cp} = logic $'1'$ and inductor currents increase. When a sensed inductor current, eg. phase A current, reaches the ramp signal $V_m - (V_m/\tau)\cdot t$ in Fig. 2(a), where τ is the time constant of integrator that is the product of resistance and capacitance in Fig. 2(a)), the corresponding flip-flop is reset to zero and Q_{ap} = logic $'0'$. Then, the inductor current starts to decrease and the on-time of the corresponding switch is determined. From Fig. 2(b), the following equation holds for all three phases in each switching cycle:

$$V_m - \frac{V_m}{\tau}\cdot t = R_s\cdot i_{Lapk}, \qquad t = D_{an}\cdot T_s.$$

Set the time constant of the integrator $\tau = K_1\cdot T_S$, where T_S is the switching period and K_1 is a positive constant. The above equation is reduced to

$$R_s\cdot i_{Lapk} = V_m - V_m\cdot\frac{D_{an}}{K_1}.$$

The proposed diagram in Fig. 2(a) realized the control key (19) for unity PFC. As a result, the phase current will follow the phase voltage and unity power factor is achieved. For convenience, K_1 is chosen to be 0.5. In this case, the carrier $V_m - V_m\cdot(t/K_1\cdot T_S)$ is symmetric to the x axis.

For the boost rectifier in Fig. 1(a), the control of switches in each leg, such as S_{an}, S_{ap}, are complementary. Due to the finite switching speed, both switches in one leg may be ON during commutation interval. Thus, the dc capacitor will be discharged through the two switches and a short through current will occur, resulting in failure of the converter. In order to prevent short circuit during the commutation time, a dead time for the complementary switches such as S_{an}, S_{ap} is implemented. Furthermore, because the energy flows only from the ac to dc side in PFC application, a dc block diode may be inserted in the dc bus of the topology in Fig. 1(a) to provide safer operation. The schematic for the power stage is shown in Fig. 3.

III. Stability Consideration

With the proposed approach, the inductor current may experience a large distortion at light load. It is found that, in certain regions of the line cycle, the inductor current could be "partly uncontrolled." From (19), the signal V_m reflects the power level of the rectifier. The higher V_m is, the larger current will flow to the load and the higher power will be delivered. The "partly uncontrolled" phenomena occurs when V_m is small and load is light (for example, 10% of nominal load). The open-loop simulation under this condition is shown in Fig. 4, when the output voltage feedback compensator is disabled and a constant reference voltage is applied to node V_m), where $V_m\cdot(1-(t/0.5\cdot T_s))$ is the carrier, $R_s\cdot i_{La}$, $R_s\cdot i_{Lb}$, and $R_s\cdot i_{Lc}$ are the sensed inductor currents, and Q_{an} Q_{bn} Q_{cn} are driving signals for switches S_{an}, S_{bn}, and S_{cn}, respectively. Simulation conditions are as follows: the input inductance is 1 mH; the switching frequency is 10 kHz; the current sensing resistance is 0.2 Ω; the output voltage is 500 V, and the voltage V_m = 1 V. Fig. 4(a) shows the switching cycle operation waveforms and Fig. 4(b) shows the line-cycle inductor current. In this case, the sensed signal $R_s\cdot i_{La}$ is above the envelope of carrier signal $V_m\cdot(1-(t/0.5\cdot T_s))$, which indicates uncontrolled operation in a small region.

The reason for this uncontrolled operation is due to the redundancy of switching states during each switching cycle. In the beginning of each switching cycle, all the lower switches S_{an}, S_{bn}, S_{cn} are turned on and the equivalent circuit is shown in Fig. 5(a). Near the end of the switching cycle when all of these three switches are turned off, all the upper leg switches S_{ap}, S_{bp}, S_{cp} are turned on. The equivalent circuit is shown in Fig. 5(b). The electrical property for these two states is identical to each other and the equivalent circuit for both cases is shown in Fig. 5(c). For both cases, the inductor

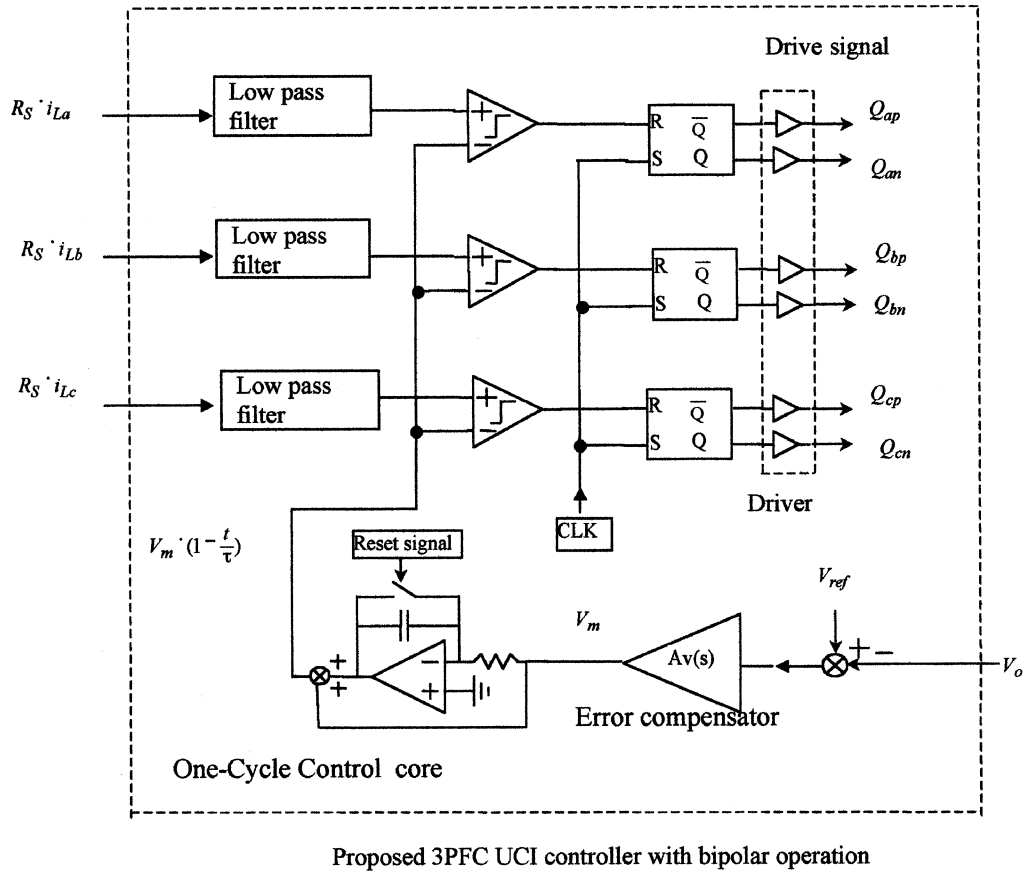

Proposed 3PFC UCI controller with bipolar operation

(a)

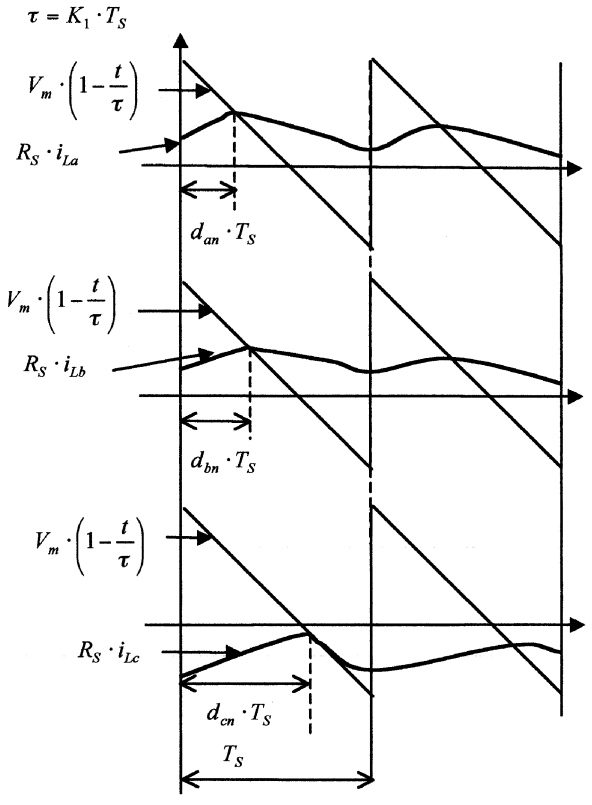

(b)

Fig. 2. (a) Schematic of proposed UCI controller for three-phase PFC with peak inductor current sensing. (b) Operating waveforms.

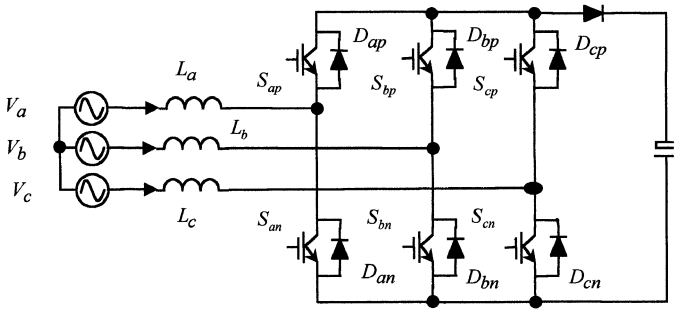

Fig. 3. Three-phase six-switch boost rectifier with a dc diode.

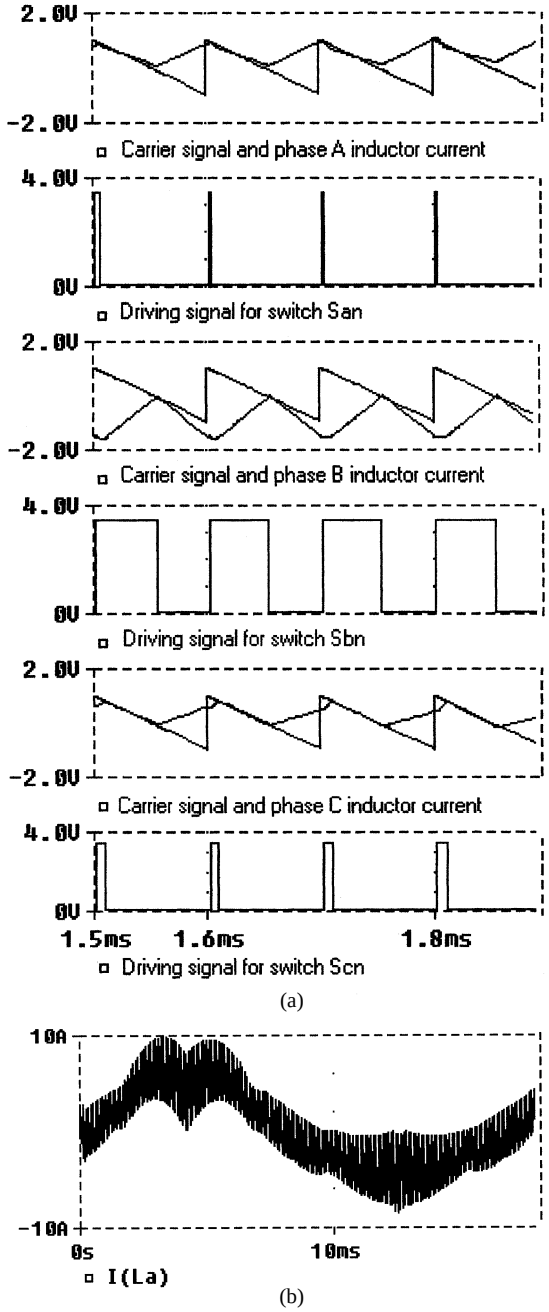

Fig. 4. (a) Simulated waveforms when inductor current is "partly uncontrolled." (b) Phase A inductor current.

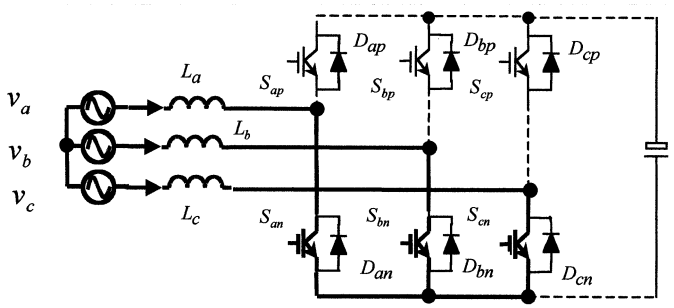

(a)

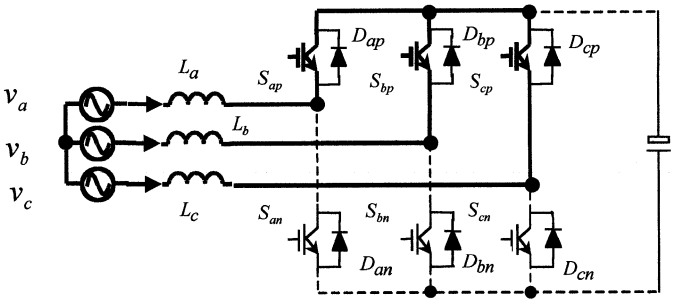

(b)

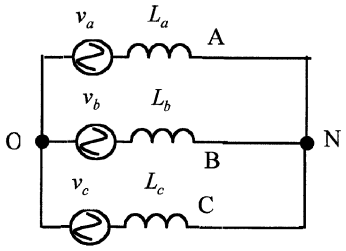

(c)

Fig. 5. Equivalent circuit (a) when three lower leg switches are turned on or (b) when three upper leg switches are turned on. (c) Equivalent circuit.

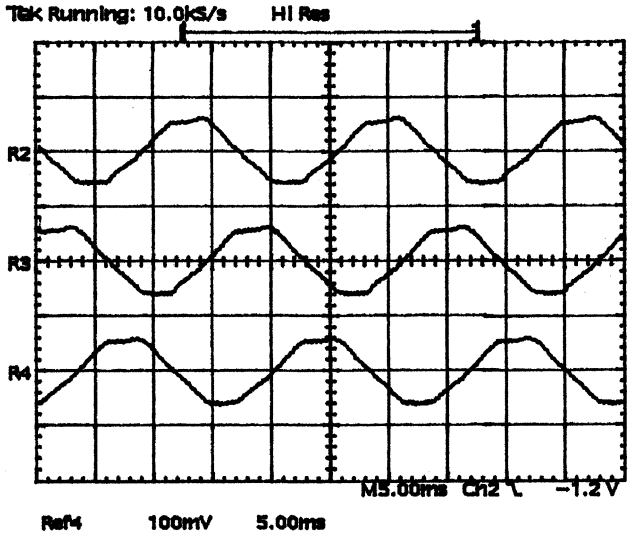

Fig. 6. Three-phase inductor current waveforms. R2: i_{La}, 5 A/div. R3: i_{Lb}, 5 A/div. R4: i_{Lc}, 5 A/div.

voltage equals phase voltage and inductor currents increase. Take phase B as an example as shown in Fig. 4(a). When S_{bn} is off, the inductor current i_{Lb} increases with a slope of $v_b\,(t)/L$ (at this time, phase v_b is negative).

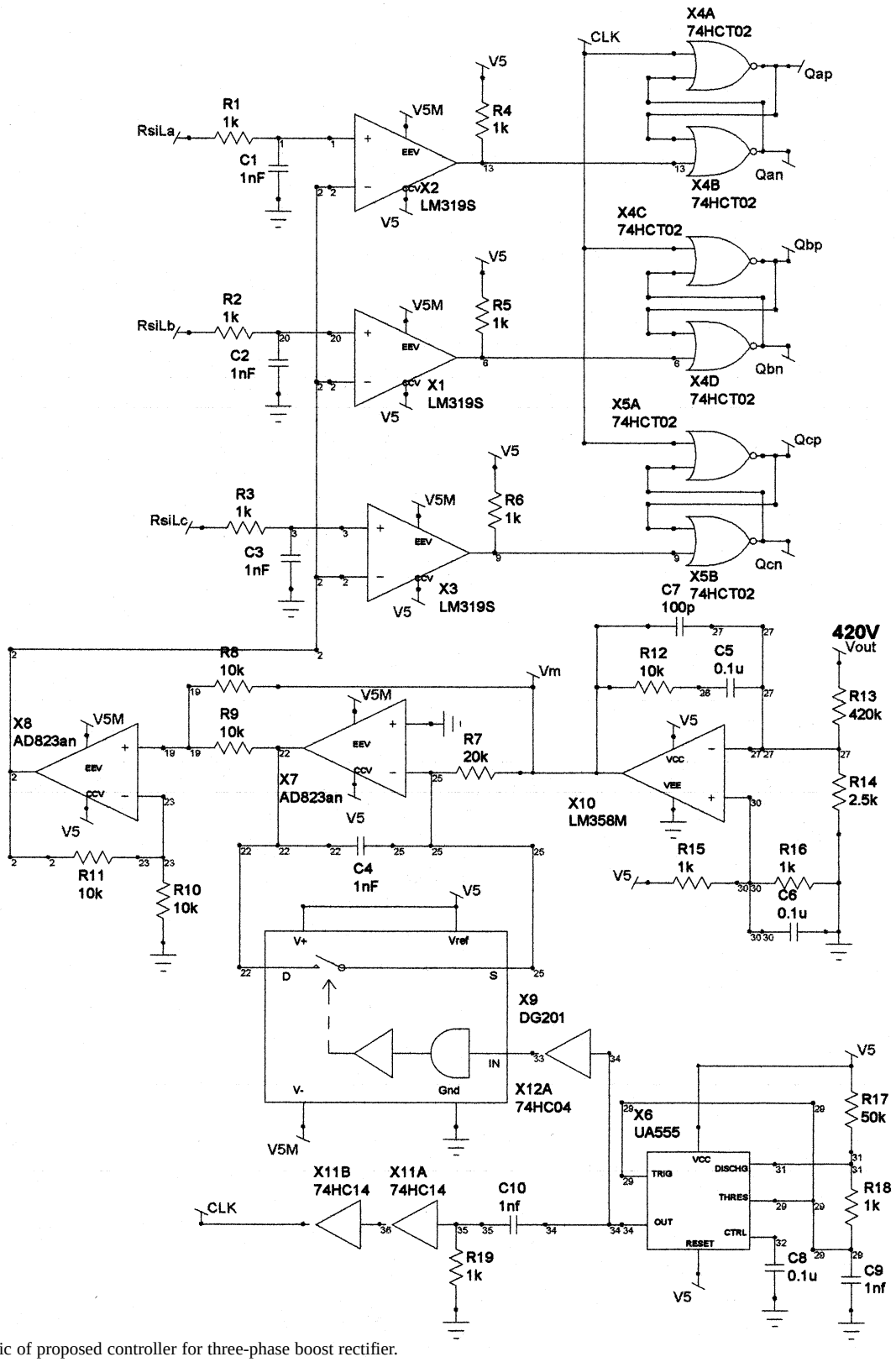

Fig. 7. Schematic of proposed controller for three-phase boost rectifier.

If the slope of inductor current is greater than the equivalent slope of ramp signal $V_m \cdot (1 - (t/0.5 \cdot T_s))$, the current will grow beyond the envelope. To avoid this situation, a circuit limitation is required, that is,

$$R_s \cdot \frac{v_b(t)}{L} \leq \frac{V_m}{\tau}.$$

The inductor should be chosen according to (20)

$$L \geq R_s \cdot \frac{V_{g\max}}{\min(V_m)} \cdot \tau \tag{20}$$

where R_s is the current-sensing resistance; $V_{g\max}$ is the peak of the input phase voltage; τ is the integration time constant (in this

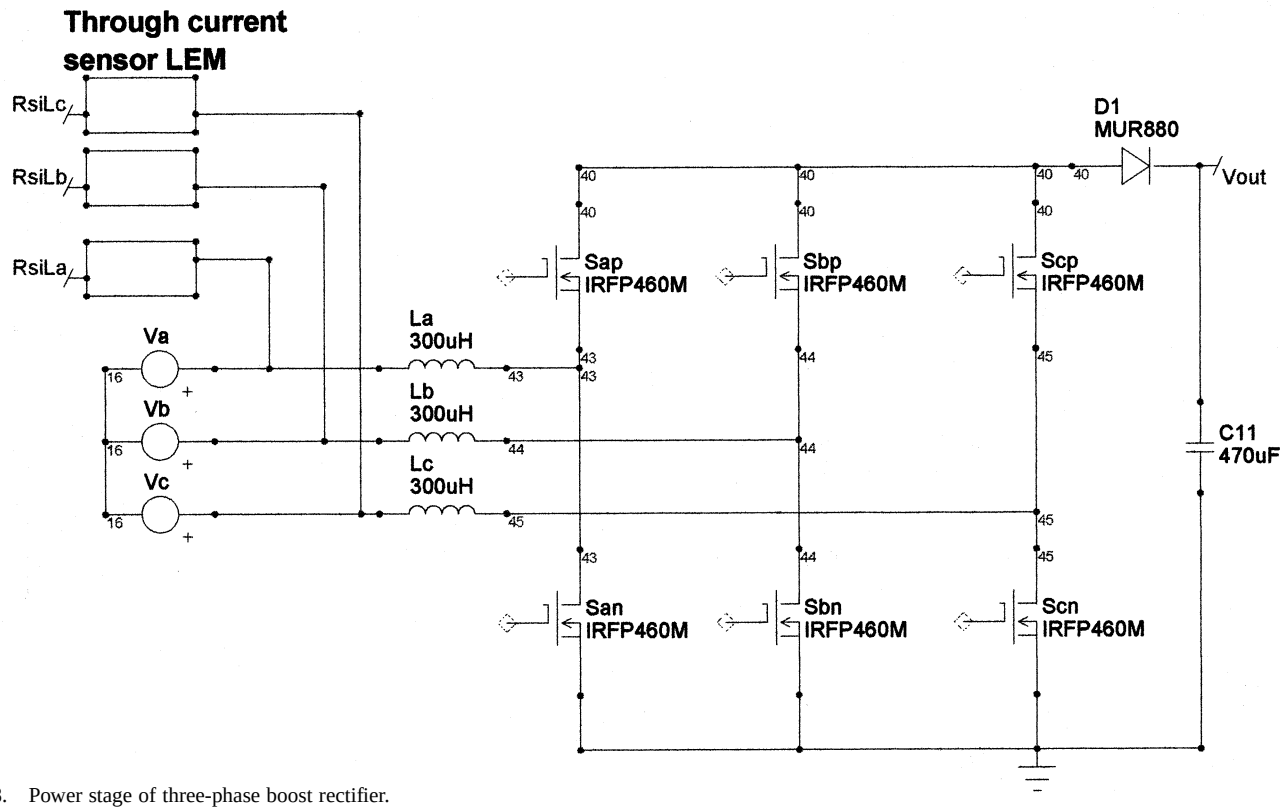

Fig. 8. Power stage of three-phase boost rectifier.

paper, τ is chosen as $\tau = 0.5T_s$); and $\min(V_m)$ is the minimum voltage of V_m as determined by the minimum load through (17).

IV. Experimental Verification

In order to verify the proposed control method, an experimental circuit was built that employs the three-phase boost rectifier, with a dc diode as in Fig. 3. The experimental waveforms are shown in Fig. 6. The real schematic is shown in the Appendix . The parameters are as follows: the inductance for inductors L_a, L_b, L_c is 300 μH; the switching frequency is 50 kHz. The input voltage is 90 Vrms. The output voltage is 420 V. The output resistance is 327 Ω and output power is 540 W. The measured input current THD is 7.5% while the input voltage has about 4% THD itself.

V. Conclusion

In this paper, a three-phase six-switch boost rectifier was investigated. The relationship between input phase voltages, output dc voltage, and switch duty ratios is given by a singular equation. Based on one of solutions and using one-cycle control, a UCI controller is proposed to achieve three-phase unity power factor. This controller employs constant frequency modulation, which is desirable for industrial applications. It is composed of one integrator with reset, along with a few linear and logic components. No multipliers and input voltage sensors are used. Nearly unity power factor was demonstrated experimentally in all three phases using this simple control circuit. Input current distortion is higher for light-load operation.

Appendix
Circuit Schematic of Three-Phase Boost Rectifier With Proposed Controller

See Figs. 7 and 8.

References

[1] P. D. Ziogas, "An active power factor correction technique for three-phase diode rectifiers," *IEEE Trans. Power Electron.*, vol. 6, pp. 83–92, Jan. 1991.

[2] J. W. Kolar and F. C. Zach, "A novel three-phase utility interface minimizing line current harmonics of high power telecommuncations rectifiers modules," *IEEE Trans. Ind. Electron.*, vol. 44, pp. 456–467, Aug. 1997.

[3] J. C. Salmon, "Comparative evaluation of circuit topologies for 1-phase and 3-phase boost rectifiers operated with a low current distortion," in *Proc. Canadian Conf. Electrical and Computer Engineering*, vol. 1, 1994, pp. 30–33.

[4] J. C. Salmon and E. Nowicki, "Operation, control and performance of a family of high power unity power factor rectifiers," in *Proc. Canadian Conf. Electrical and Computer Engineering*, 1995, pp. 854–857.

[5] H. Mao, D. Boroyevich, and F. C. Lee, "Analysis and design of high frequency three-phase boost rectifiers," in *Proc. IEEE APEC'96*, 1996, pp. 538–544.

[6] K. Smedley and S. Cuk, "One-cycle control of switching converter," in *Proc. IEEE PESC'91*, Cambridge, MA, June 24–27, 1991, pp. 888–96.

[7] Z. Lai and K. M. Smedley, "A general constant frequency pulse-width modulator and its applications," *IEEE Trans. Circuits Syst. I*, vol. 45, pp. 386–396, Apr. 1998.

[8] C. Qiao and K. M. Smedley, "A general three-phase PFC controller. Part I for rectifiers with a parallel-connected dual boost topology," in *Conf. Rec. IEEE-IAS Annu. Meeting*, Oct. 1999, pp. 2504–2511.

[9] ——, "A general three-phase PFC controller. Part II for rectifiers with a series-connected dual boost topology," in *Conf. Rec. IEEE-IAS Annu. Meeting*, Oct. 1999, pp. 2512–2519.

[10] K. M. Smedley and C. Qiao, "Unified constant-frequency integration control of three-phase rectifiers, inverters, and active power filters for unity power factor," U.S. Patent 6 297 980, Oct. 2, 2001.

Chongming Qiao (S'98) was born in Taiyuan, China, in 1969. He received the B.S degree in electrical engineering from Xi'an Jiaotong University, Xi'an, China, in 1991, and the M.S degree in power electronics from Zhejiang University, Hangzhou, China, in 1994. He is currently working toward the Ph.D. degree in the Power Electronics Group, University of California, Irvine.

His research interests include single-phase and three-phase power-factor correction, active power filters, and single-phase single-stage power-factor correction.

Keyue Ma Smedley (S'87–M'90–SM'97) received the B.S. and MS. degrees from Zhejiang University, Hangzhou, China, in 1982 and 1985, respectively, and the Masters and Ph.D. degrees from California Institute of Technology, Pasadena, in 1987 and 1991, respectively, all in electrical engineering.

She was an Engineer at the Superconducting Super Collider from 1990 to 1992, where she was responsible for the design and specification of ac–dc conversion systems for all accelerator rings. In 1992, she joined the Faculty of Electrical and Computer Engineering, University of California, Irvine, where she established the state-of-the-art Power Electronics Laboratory. Her research interests include control, topologies, and integration of dc–dc converters, high-fidelity class-D power amplifiers, active and passive soft-switching techniques, single-phase and three-phase power-factor correction and active power filter methods, and grid-connected inverters for alternative energy sources.

Dr. Smedley is an At-Large AdCom member of the IEEE Power Electronics Society, the Chair of the Constitution and Bylaws Committee of the IEEE Power Electronics Society, an Associate Editor of the IEEE TRANSACTIONS ON POWER ELECTRONICS, a faculty member of Eta Kappa Nu, and a member of the Power Sources Manufacturer's Association. She was the Chair of the IASTED and IEEE Power Electronics Society cosponsored International Symposium on Power Generation and Renewable Energy Sources in 2002.